# An EcosimPro Model of a Power Processing Unit for a Low Power Hall Effect Thruster

**A. Sollazzo[(1)], D. Ricci[(2)], P. Natale[(3)], F. Battista[(3)],**

*[(1)] Environmental Acoustics & Pollutant Emissions Lab.,*
*[(2)] Electric Propulsion Facility Lab., [(3)] Space Propulsion Lab.*
*Italian Aerospace Research Centre, Via Maiorise, snc – 81043 Capua (CE), Italy*

**KEYWORDS:** Electric Propulsion, Power-processing Unit, Hall Effect thruster, Modelling.

**ABSTRACT:**

CIRA has recently launched the IMP-EP project, aiming at improving the design, diagnostics and testing capabilities on Electric Propulsion issues. In particular, the Hall Effect thruster technology has been chosen and an engine, belonging to 250W-class is currently under development. In this view, preliminary studies on the Power Processing Unit have been started. This paper describes a simplified model of a Power Processing Unit, for a Hall Effect Thruster, implemented in the EcosimPro modelling environment. The model concerns the power converters of the three channels for the thruster operation, along with their respective control systems as well as their proper modulators. The model has been tested by attaching it to a steady state representation of the thruster, to reproduce proper power consumption for each selected condition.

## 1. INTRODUCTION

CIRA, the Italian Aerospace Research Center, endorsed by ASI, has recently launched a new project (IMP-EP), acting to support the National and European companies in R&D activities, and giving a significant contribution to the present technology maturation (in particular, HET) [1]. Within this framework, CIRA intends to play a significant role in the EP technology development, extending and even improving the capabilities in terms of design, diagnostics, manufacture and test of electric thrusters. In fact, present European capability tops at about 5 kW thruster power level; however, most future mission scenario for EP-enhanced space transportation of large payloads foresee the use of thrusters, characterized by power higher than 10 kW. CIRA drew up a plan aiming at realizing two facilities: the Medium Scale Vacuum Chamber (MSVC), i.e. 2 m of diameter and 5m long, conceived to implement first testing capabilities and allow for the R&D on engines, characterized by power up to 5 kW; the Large Scale Vacuum Chamber (LSVC), representing a world-class test facility (i.e. 8 m of diameter and 16m long). On the low-power-engine line side, the realization of a facility, suitable for the R&D activities on engine with power values up to 5 kW, together with the manufacturing of a 250W-class-power thruster, as first design implementation, is foreseen by the end of 2017. In this framework, the preliminary studies on the Power Processing Unit have been started, adopting engineering tools, as EcosimPro [2].

The EcosimPro modelling environment can be improved by means of a proper space propulsion library supported by European Space Agency (ESA). This library, called European Space Propulsion System Simulation (ESPSS), already foresees both a thruster and a PPU model [2]. Anyway, the model, here reported, is intended to reproduce the power converters behavior with higher details level in order to take into account the distortion of all the electrical quantities and to model the interactions between the thruster and the PPU.

The paper is organized as follows. The first section is the introduction to paper while second section describes the general model architecture and then gives the details of the three drivers of the thruster operating channels. Third section reports the selected case studies and corresponding numerical results. Fourth section summarizes the author's conclusions, the outcomes of the modelling activity and discusses the future work.

## 2. ACTIVITIES BACKGROUND

According to CIRA vision, some test articles will be developed in order to implement capabilities in

terms of comprehension of physical phenomena, facility and diagnostics operations. They will be tailored on MSVC and LSVC testing performances [3]. In this context, CIRA has the objective of developing a low power class thruster (hundreds of watt class) and a high power class thruster (tens of kilowatt). The thruster architecture, selected for the development activities, are the Hall Effect thrusters, due to their scalability and the scientific community interest [1]. Both thrusters will follow a technology development phase where different mock-up models will be produced and tested at different levels.

Currently the low power class thruster (a nominal power of 250 W has been selected) is in a Preliminary Design Review Phase and have been designed according to the criteria reported in [4]. The preliminary version of the thruster, having an external diameter of 80 mm, is reported in the following picture. The high power thruster is currently in the conceptual design phase.

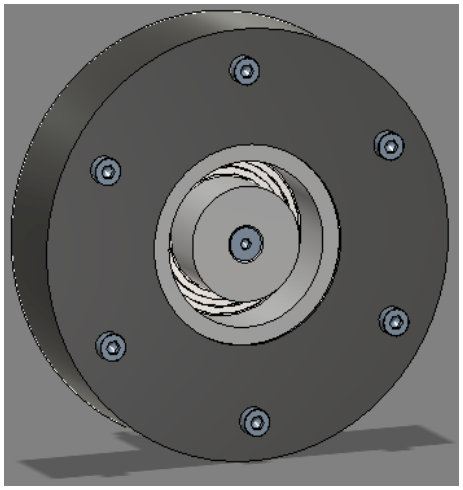

*Figure 1. Preliminary design of CIRHET-250*

## 3. ARCHITECTURE OF MODEL

In Figure 2, the first level architecture of the PPU model is reported. It is evident how the four drivers are connected in parallel and supplied by an ideal DC voltage power source [5], [6]. This choice is for the sake of simplicity, and anyways it does not withdrawn the value of the model in terms of power quality modelling. The bus voltage is a conventional 28 V voltage [5], [6]. It supplies the discharge channel, the cathode heater and the cathode ignitor/keeper.

Each control channel of the thruster can be considered as an adjustable electrical generator, depending on the regulated electrical quantity [7]. Indeed, the anode discharge driver forces the desired voltage level, thus it is considered a voltage generator. Instead, the two remaining drivers impose the respective desired currents to their loads, so they are represented as two adjustable currents generators.

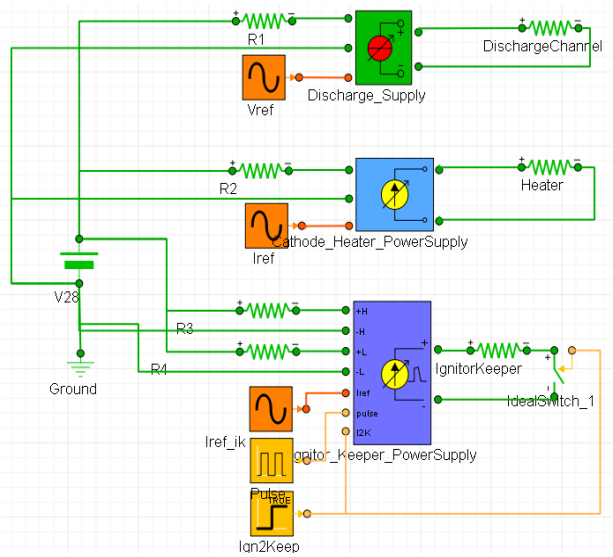


*Figure 2. First level architecture of PPU model.*

It is also evident the simple representation of each of thruster operational channel. Only the power consumption in steady state conditions is represented for heater and anode discharge, while the variation of ignitor/keeper load is represented at least in the two stable conditions of open circuit, before discharge takes place, and steady state resistive behavior, for keeper mode after cathode discharge has been activated.

The model foresees a control system [8] with a proper modulator [7] for regulating the electrical quantity of interest for the given thruster channel. The general scheme of each driver of thruster channels is shown in the following Figure 3.

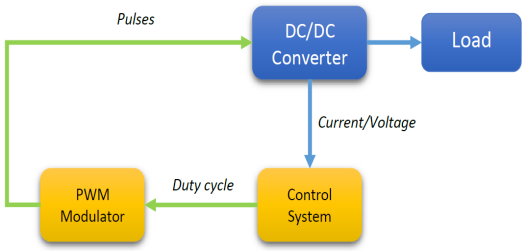


*Figure 3. General scheme of each thruster channel driver*

In the next subsections, the details of each thruster driver are reported.

### 3.1. Anode Discharge Driver

The anode discharge channel represents the main channel in terms of power consumption [5]. Moreover, anode current regulation directly allows thrust regulation. These two features makes the anode discharge the main control channel. Figure 4 depicts the logical scheme of driver and related control [9].

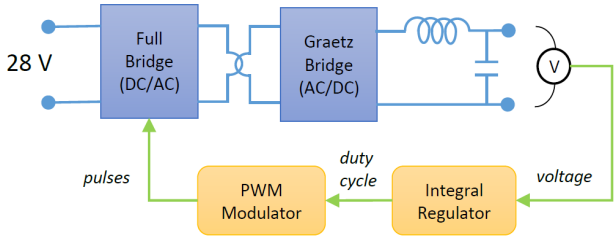


*Figure 4. Anode discharge driver and control scheme*

The regulated quantity is the output voltage. The integral controller produces the control variable, representing the phase-shift between the two pulses trains used to activate the power switches of the full-bridge [7]. Figure 5 shows the circuit schematics of the driver. The two switches of a leg (EPWM1A/B and EPWM2A/B) are complementary activated if death-time is neglected. Now, the phase-shift of the two pulses trains, up for half a period and down for the remaining time, drive the two legs switches and control the RMS of output transformer voltage. Indeed, a zero delay (two upper/lower switches open and closed in the same time) produces a null voltage, while a half-period delay produces maximum RMS of output voltage. Finally, the diodes bridge and the LC filter rectifies and stabilizes the output voltage.

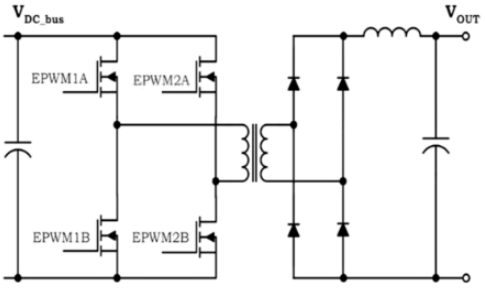


*Figure 5. Circuit schematics of anode discharge driver*

Table 1 reports the parameters of anode discharge driver.

*Table 1.Parameters of anode discharge driver*

| Parameter | Value |
|---|---|
| Input voltage ($V_{in}$) | 28 V |
| Transformer ratio ($V_1/V_2$) | 7/100 |
| Filter inductance (L) | 20 mH |
| Filter capacitance (C) | 40 nF |
| Switching frequency ($f_{sw2}$) | 20 kHz |

### 3.2. Heater Driver

The cathode heater is the electrical component used to let the inner liner of hallow cathode reach the proper temperature to start the thermionic electron emission. The emitted electrons produce ionization of gas insufflated in the cathode insert region. Once the physical and chemical conditions make the plasma production process to hold by itself, heater turns off.

Figure 6 depicts a possible scheme [10] for cathode heater driver along with its control system. The selected driver is a push-pull converter. The two power switches are operated by two trains of pulses obtained starting from the same signal and applying to the second a phase-shift by an half of period. The up time of the two signals is regulated by the duty cycle and varies between zero, producing null output voltage, and an half of period, producing the maximum output voltage. The two switches alternatively connect the DC input voltage to the semi-winding of transformer with central plug, and then the turns ratio adjusts the voltage level and the diodes rectifier produce a DC voltage with a ripple superimposed. Finally, the output filter reduces the ripple value.

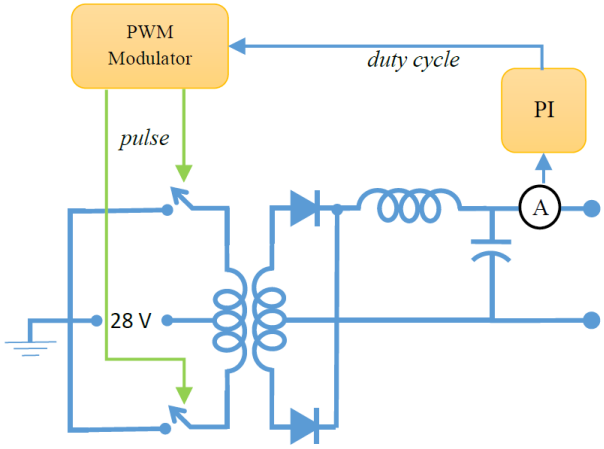


*Figure 6. Heater driver and control scheme*

The heater driver transfers power to its load, for heating the inner cathode liner, by regulating the desired current, thus the control scheme feedbacks and regulate this quantity. Table 2 reports the circuital parameters of the driver here described.

*Table 2.Parameters of heater driver*

| Parameter | Value |
|---|---|
| Input voltage ($V_{in}$) | 28 V |
| Transformer ratio ($V_1/V_2$) | 1/1 |
| Filter inductance (L) | 0.5 mH |
| Filter capacitance (C) | 12 μF |
| Switching frequency ($f_{sw3}$) | 20 kHz |

### 3.3. Ignitor and Keeper Driver

The ignitor and keeper driver has the twofold task to operate in two mutually active modes. First, the ignitor is in charge to activate the discharge in cathodic plasma by applying very high voltage pulses, and then keeper undertakes to hold electronic current active to feed anode and to neutralize plume electric charge.

Figure 7 shows the schematic of the drive [11], mainly evidencing the voltage pulse generator of ignitor. The keeper portion of driver is the boxed Full-Bridge and Graetz's Bridge, whose behavior has already been described in subsection 3.1, while explaining anode discharge driver. Full-Bridge and Graetz's Bridge control and operation have already been discussed as well. The only difference here is that the quantity regulated is the output current instead of voltage.

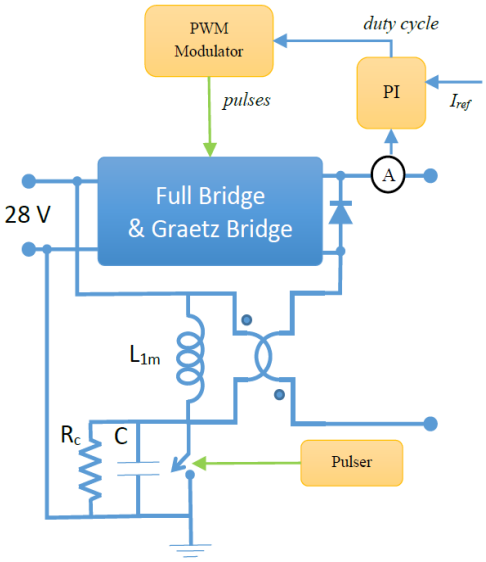


*Figure 7. Ignitor and Keeper drivers and control scheme*

The voltage pulses generator [12], in fact, has a structure very similar to a boost converter, but its aim is to produce the proper pulse on the secondary winding of transformer, when the power switch opens. In this phase, the energy stored in the equivalent magnetizing inductance of transformer, when the switch was closed, rapidly passes to the capacitor. The already mentioned voltage pulse is amplified by means of turns ratio of transformer to the secondary winding and force the diode in parallel to the other converter to conduct, thus transferring part of the energy to the load. This way the keeper mode converter is short-circuited. In this phase, discharge is not active yet, thus the ignitor driver substantially works with an open circuit load.

On the other hand, when discharge is finally triggered, the ignitor switch operation is turned off and the keeper converter start to work for holding the cathodic current. It is worth to remark here that the keeper converter does not foresees an inductor in its output filter. Anyway, the ignitor transformer is successfully exploited for the keeper current smoothing. The circuit parameters are reported in the following Table 3 and Table 4.

*Table 3. Parameters of keeper driver*

| Parameter | Value |
|---|---|
| Input voltage ($V_{in}$) | 28 V |
| Transformer ratio ($V_1/V_2$) | 7/10 |
| Filter capacitance (C) | 0.1 mF |
| Switching frequency ($f_{sw3}$) | 20 kHz |

*Table 4. Parameters of ignitor driver*

| Parameter | Value |
|---|---|
| Input voltage ($V_{in}$) | 28 V |
| Transformer ratio ($V_1/V_2$) | 1/5 |
| Magnetization inductance ($L_m$) | 10 mH |
| Storage Capacitance (C) | 150 μF |
| Discharge Resistance ($R_c$) | 0.5 kΩ |

Finally, the control system of the keeper part of the circuit is a classic PI controller [8], while pulses generator controller is here represented by a simple logical pulse generator to operate the switch. Parameters of ignitor pulser are summarized by Table 5.

*Table 5. Parameters of ignitor pulser*

| Parameter | Value |
|---|---|
| Pulse period ($T_p$) | 0.1 s |
| Pulse duration ($t_d$) | 10 ms |

The dynamics of discharge start are not represented in the presented model, as well as the automatic switch between the two operational modes of the driver. Only a time driven change of operative mode is represented so far.

## 4. NUMERICAL SIMULATIONS

This section reports the numerical simulations carried out to test the behavior of the PPU model. Two case studies are here reported to evaluate the PPU model performances. The data of each of them are reported in Table 6.

*Table 6. Case studies parameters.*

| Case study (1): top power | | |
|---|---|---|
| *Channel* | *Demand* | *Power Consumption* |
| Anode discharge | 300 V | 255 W |
| Heater | 2 A | 24 W |
| Keeper | 0.25 A | 10 W |
| Case study (2): middle power | | |
| *Channel* | *Demand* | *Power Consumption* |
| Anode discharge | 300 V | 150 W |
| Heater | 2 A | 24 W |
| Keeper | 0.25 A | 10 W |

The case studies concerns two conditions for the anode discharge channel, which locates, the first, in the top and the second in a middle level in terms of power consumption.

Both simulations foresee the same activation sequence [6] of the thruster driver to more realistically represent an actual starting sequence of an HET. Anyway, the timing simulated is very short, only 200 ms, for time simulations saving, thus delays between activation instants of each driver are very short. The order of firing considers first of all heater, for producing cathodic plasma, then ignitor starts pulsing, to activate discharge in the cathode, after the second pulse it is assumed the discharge as active and the keeper is started. After a few, to let keeper reach steady state, anode discharge driver is triggered. Details on the sequence are reported in Table 7.

*Table 7. PPU starting sequence*

| Driver | Start time (s) |
|---|---|
| Heater driver | 0.002 |
| Ignitor | 0.032 |
| Keeper | 0.145 |
| Anode discharge diver | 0.160 |

Following figures shows main electrical quantities waveform for the two simulated conditions. Figure 8 shows the heater current for both top and middle power simulated conditions. Both control goals of fast dynamics and steady state stability are achieved. Ripple value is bounded in a ±3% range, which is a good results if compared to literature requirements [5], even though it refers to an higher power thruster. While investigating in details the waveform, it evidences that ripple is mainly caused by a sinusoidal component whose location in frequency is nearby 2 kHz. Although a more detailed spectral analysis should be carried out to confirm that fact, the observed component is not a characteristic one for the heater driver, and it is probably due to the interaction with the other converters [12].

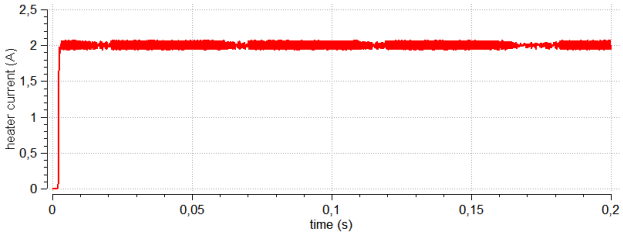


*Figure 8. Heater current for case studies (1) and (2)*

Figure 9 reports ignitor output voltage. Only two pulses are simulated, but it is enough to assess the proper behavior of the driver if compared to [10].

Moreover, the voltage peaks are very close to the desired value of 1.2 kV.

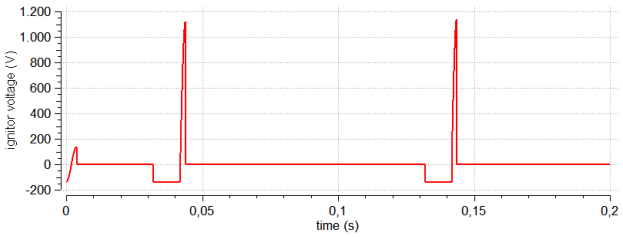


*Figure 9. Ignitor voltage for case studies (1) and (2).*

The keeper current is reported in Figure 10 and it is exactly as expected. Control requirements, concerning dynamics and steady state, are fulfilled. It is evident how ripple level is almost negligible, so interactions with the other converters are properly filtered.

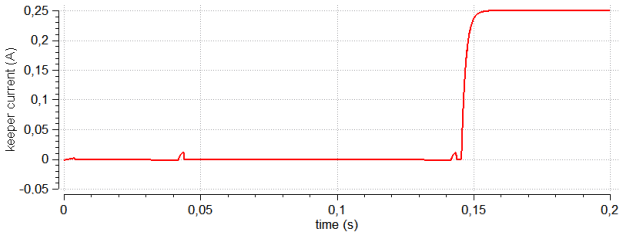


*Figure 10. Keeper current for case studies (1) and (2)*

The anode discharge voltage is shown in Figure 11 and it is compliant to what is expected. Ripple level is below ±1.5%, and that is particularly good if compared to typical requirement [5], but surely the simulated load is extremely friendly.

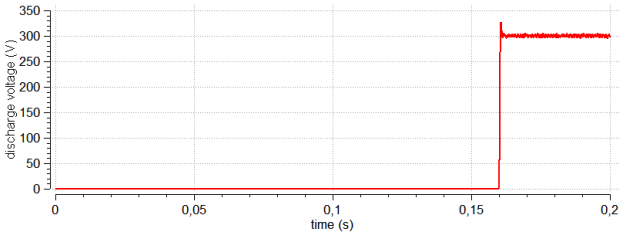


*Figure 11. Anode discharge voltage for case studies (1) and (2)*

Current from anode discharge channel is of course proportional to voltage, due to the adopted model of load. Anyway, both Figure 12 and Figure 13 highlight the proper value of power, modulated to the load.

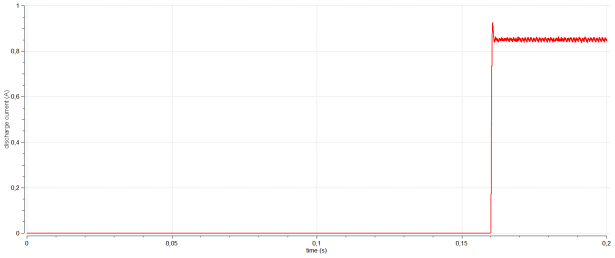

*Figure 12. Anode discharge current for case study (1)*

In general, the model exhibits a proper behavior also while representing unwanted interactions between each converter. A detailed spectral analysis for several working conditions should be necessary to better assess this point, to forecast at least the main harmonics component to compare both in terms of spectral localization and amplitude the simulated results with the foreseen data from assessed literature [12].

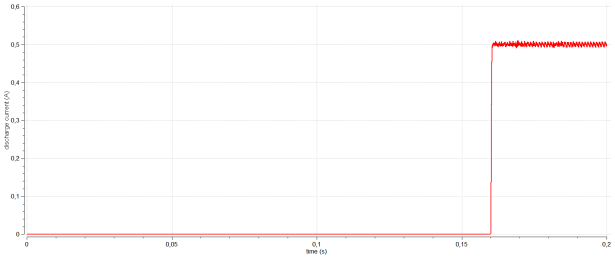

*Figure 13. Anode discharge current for case study (2)*

## 5. CONCLUSIONS

A PPU simplified model for an HET, implemented in EcosimPro modelling environment has been presented. The reference HET model is the thruster, under development in CIRA. The model shows proper behavior concerning the main electrical quantities. Moreover, the interactions between the power converters used to drive the three channels of the thruster are represented.

Even though the first version of a PPU shows good modelling performances, it still lacks mainly a proper model for the bus power supply. Further, several circuital elements, necessary to represent a more realistic behavior, such as snubbers, current limiters and so on should be taken into account. Finally, a detailed spectral analysis should be

carried out to assess the correctness of the harmonics and interharmonics content of each of the electrical quantities.

## 6. REFERENCES


1. Salvatore, V., Battista, F., Ricci, D. & Invigorito, M. (2015). CIRA Development Activities in Electric Propulsion Testing. In Proc. of 66th International Astronautical Congress, Jerusalem, Israel, paper n. IAC-15,C4,4,12,x29892.
2. ECOSIMPRO User's Guide, EA Internacional, Magallanes, Madrid, Spain.
3. Invigorito, M., Ricci, D., Battista, F. & Salvatore, V. (2016). CIRA Roadmap for the Development of Electric Propulsion Test Facilities. In Proc. of Space Propulsion 2016, May 2-6, Rome, paper n. SP2016_3125134.
4. Battista, F., De Marco, E.A., Misuri, T., & Andrenucci, M. (2007). A Review of the Hall Thruster Scaling Methodology. In Proc. 30th International Electric Propulsion Conference (IEPC 07). IEPC-2007-313.
5. Hamley, J.A., et al. (1993). Power Electronics Development for the SPT-100 Thruster. In Proc. IEPC-1993.
6. Fisher, G. et al. (1993). Design of a High Efficiency Power Processor for the Russian Stationary Plasma Thruster. In Proc. of the IEPC-1993
7. Mohan, N., Undeland, T.M., & Robbins, W. P. (2002). Power Electronics: Converters, Applications, and Design. Wiley&Sons.
8. Astrom, K.J. (2002). Lectures of Control Systems Design. Caltech Reports.
9. Piñero, L. R., et al. (2002). High Performance Power Module for Hall Effect Thrusters. In Proc. of 38th AIAA/ASME/ SAE/ASEE Joint Propulsion Conference and Exhibit, Indianapolis, Indiana, July 7- 10
10. Hamley, J.A., et al. (1993). Development of a Power Electronics Unit for the Space Station Plasma Contactor. In Proc. of IEPC-1993
11. Hamley J. A., & Hill, G. M. (1991). Power Electronics for Low Power Arcjets. In Proc. of 27th Joint Propulsion Conference.
12. Sarmiento, C.J., Gruber, R. P. (1987). Low Power Arcjet Thruster Pulse Ignition. In Proc. of the 23rd Joint Propulsion Conference, San Diego, California, June 29-July 2.
13. De Rosa, F., Langella, R., Sollazzo, A., & Testa, A. (2005). On the interharmonic components generated by adjustable speed drives. IEEE Trans. on Power Delivery (20).